

Development of substructure in Zircaloy-4 during LCF at 873 K

I. ALVAREZ-ARMAS

C.O.N.I.C.E.T., Bv. 27 de Febrero 210 bis-2000-Rosario, Argentina

A. F. ARMAS

U.N.R., Av. Pellegrini 250-2000-Rosario, Argentina

R. VERSACI

Materials Department C.N.E.A., Av del Libertador 8250-1429-Bs.As., Argentina

Transmission electron microscopy techniques were used to study the substructure developed in Zircaloy-4 during strain controlled Low Cycle Fatigue (LCF) test at 873 K. A complete microstructural analysis on samples cycled with a total strain range of 0.01 and total strain rate $2 \times 10^{-3} \text{ s}^{-1}$ was made at a different number of cycles. This study revealed that the dislocations arranged themselves into a band structure which remains essentially constant since the first cycle up to fracture. This substructure stability agrees with the stress response observed of this alloy at 873 K. A mechanism to account for the observed structure is proposed.

1. Introduction

Studies of the substructure developed during reversed cyclic deformation were one of the main subjects of investigations in fatigue during the last years. However the correlation between a determined mechanical behaviour and its corresponding dislocations structure remains not clear.

For face centered cubic metals, where the major of investigations were performed [1, 2, 3] it is known that different types of structures can be found on performing high strain fatigue experiments at different temperature. If a single slip system predominates, a very regular wall structure results. When multiple slip systems are active, cell structures develop. On increasing temperature the cell structures change to subgrains with tightened walls and misorientation angles between them.

This high temperature structure was not observed on studying Zircaloy-4 at temperatures above the strain ageing region [4]. Instead, we have found well developed bands of dislocations in all the grains searched. To the authors knowledge, this is the first result reported in the literature about the dislocation structure developed on hexagonal closed packed metals during cyclic deformation in the high temperature range. Therefore, the aim of the present investigation was to analyse these bands and to propose a mechanism for the band formation.

2. Experimental procedure

A description of the used material, Zircaloy-4, was given in a previous publication [5]. The mean grain diameter was 20 micrometres and the preferred orientation of the grain was (11 $\bar{2}$ 0). The thin foils were prepared from sections cut perpendicular and occasionally parallel to the tensile axes. Several trans-

verse slice, about 0.2 mm thick, were sectioned from the gauge section using a thin sectioning machine. Each slice was cut into four or five 3 mm discs. These discs were rapidly electropolished with a Tenupol Electropolishing Unit. A solution of 10% perchloric acid 35% *n*-butanol and 55% methanol was used as the electrolyte. The polishing conditions were 30 V at room temperature. The dislocation substructure was studied with a JEOL 200 transmission electron microscope operated at 200 kV equipped with a double-tilt type holder.

3. Results

3.1. Typical substructure

The stress response of Zircaloy-4 for strain-controlled cycling in the range 573 to 873 K is shown elsewhere [4]. The mechanical stability observed at 873 K (Fig. 1) was correlated with the character of the dislocation structure developed during cycling, (Fig. 2). This structure turned out to be typical for the steady-

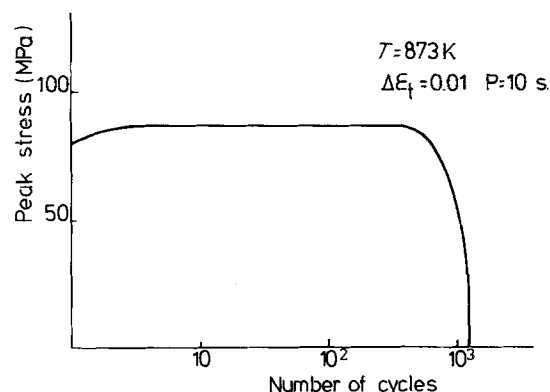


Figure 1 Peak stress response as a function of the number of cycles, $\Delta\epsilon_f = 1\%$, $T = 873 \text{ K}$.

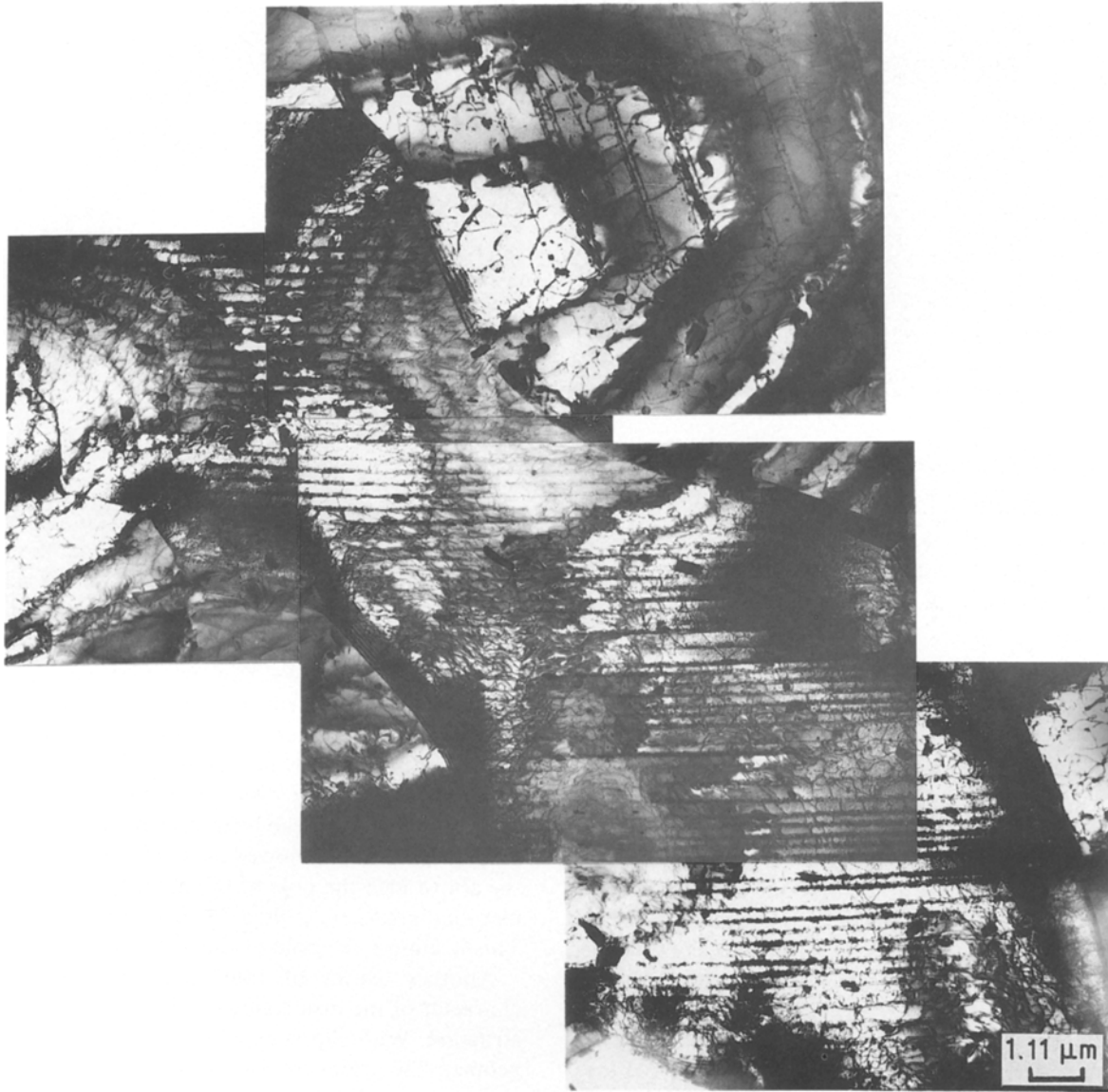


Figure 2 Dislocation substructure observed in a LCF failed specimen of Zircaloy-4 at 873 K with $\Delta\epsilon_f = 1\%$.

state deformation during high temperature fatigue. Furthermore, the same structure was observed for a specimen interrupted at 50 cycles. Microstructural observations on samples cycled at 3/4 of a cycle, (Fig. 3), have shown straight slip traces on prism plane in some grains, groups of long straight screw dislocations in others, and a high density of elongated loops lying along $\langle 0001 \rangle$ on the rest. It is worth noting that, such elongated loops are often observed on the final band structure.

Due to the material texture, all the micrographs were taken for a beam direction 30° around the $[11\bar{2}0]$ direction. In order to scan the substructure for crystallographic direction near the basal pole, longitudinal thin foils were also examined. Plentiful observations show that the present structure does not change between crystallographic directions. This homogeneous distribution of deformation agrees with the symmetrical shape of the hysteresis loops.

3.2. Burger's vector

Dislocation Burger's vector analysis were performed using the usual $\bar{g} \cdot \bar{b} = 0$ invisibility criterion, where \bar{g} is the operating reflection vector and \bar{b} is the Burger's

vector of the dislocation. In the analysis all the lines became invisible in the (0002) reflection and hence their corresponding Burger's vector are of the $\langle a \rangle$ -type. Since all the dislocations are also invisible with a $(0\bar{1}11)$ reflection but not with $(1\bar{1}00)$ and $(10\bar{1}1)$ reflection, it was concluded that the operating Burger's vector is $\frac{1}{3}(2\bar{1}\bar{1}0)$.

3.3. Trace analysis

The stereomicroscopy technique makes it possible to obtain not only a 3-dimensional picture of the substructure but also to recognise prominent planes and directions of a microstructure. Fig. 4 shows the structure viewed from two different orientations, one near $[11\bar{2}0]$ and the other near $[11\bar{2}3]$, with the same reflection plane $(2\bar{2}00)$. The specimen has therefore been tilted 55° between the recording of these two micrographs, about $[1\bar{1}00]$ which is parallel to the band direction only in the first orientation. The misorientation observed in the second one is about 15° , as can be observed in Fig. 4b. This latter determines that the band direction is not parallel to $[1\bar{1}00]$ direction.

Fig. 5 shows a set of micrographs which were taken in two-beam condition with $g = (2\bar{1}\bar{1}0)$ near

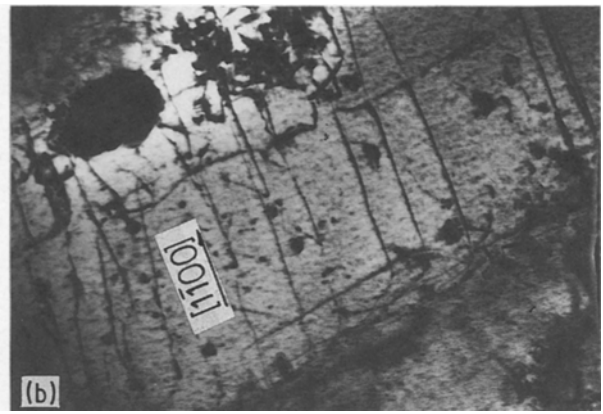
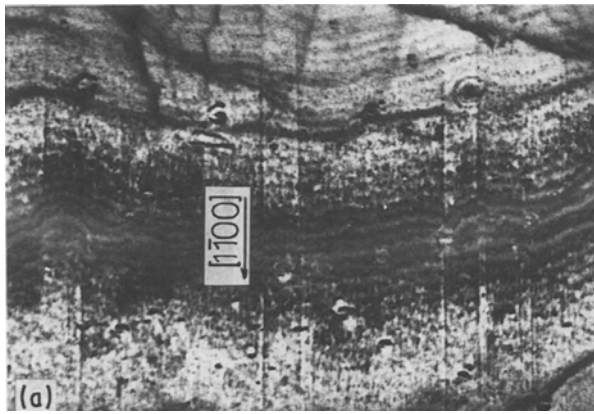
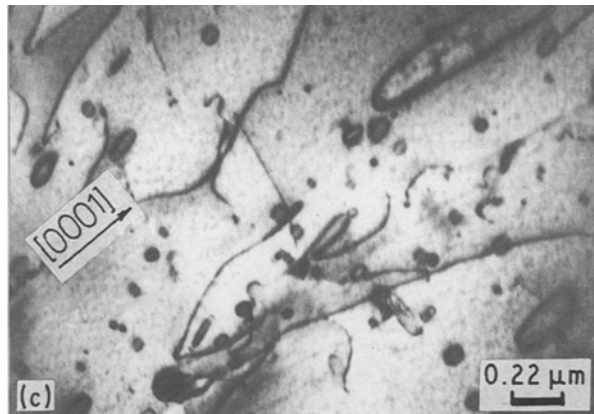


Figure 3 Dislocation substructure observed at 3/4 of a cycle.



the $[0\bar{1}12]$ zone axis in the first one and $g = (2\bar{1}\bar{1}0)$ and $g = (10\bar{1}1)$ near the $[01\bar{1}1]$ zone axis in the last two micrographs. The tilt experiment was performed about the $[2\bar{1}\bar{1}0]$ axis from $[0\bar{1}12]$ to $[01\bar{1}1]$ beam direction. Therefore the specimen has been tilted 60° . As the tilt experiment develops, the walls of the dislocation band became wider while the $[01\bar{1}1]$ crystallographic direction approaches the beam direction and the trace of the bands always remain in the same orientation. From the above experiment one can con-

clude that the Burger's vector direction coincides with the direction band. In order to estimate the habit plane of the dislocations which compose the walls, a series of stereomicrographs, similar to the last one, were analysed by means of an approximate trace analysis [6] as follows: Fig. 6a shows a schematic representation of the substructure observed in the last tilt experiment. Under the assumption that the foil plane is approximately normal to the incident electron beam, the trace of the dislocation band as well as the two-beam direction, can be transferred into the stereographic projection showed in Fig. 6b. According to the above idea the pole of the habit plane lies on the meridian great circle tilted 90° from foil normal pole. This is almost the pole of the $(01\bar{1}1)$ plane.

Another aspect of trace analysis concerns the character of the dislocations which compose the substructure. With slip occurring on the prism planes, a geometrical argument can be used to differentiate between the dislocation having an edge or screw character [7]. This is possible when a foil is viewed in a $[1\bar{1}\bar{2}0]$ or $[1\bar{1}00]$ direction, since screw dislocations

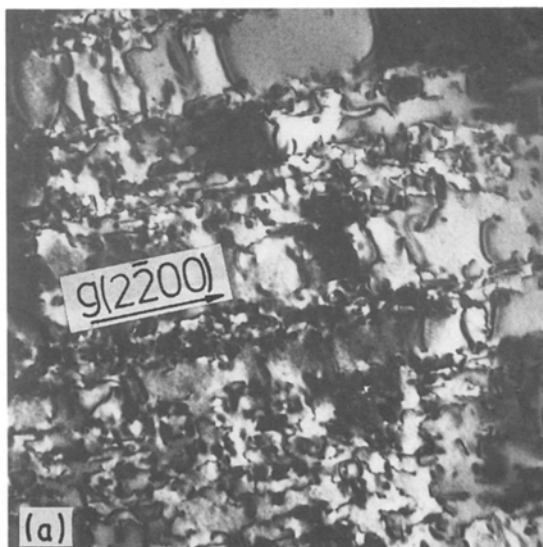


Figure 4 Tilt experiment with $[2\bar{2}00]$ axis: (a) $\bar{B} = [1\bar{1}\bar{2}0]$ and (b) $\bar{B} = [1\bar{1}\bar{2}3]$.

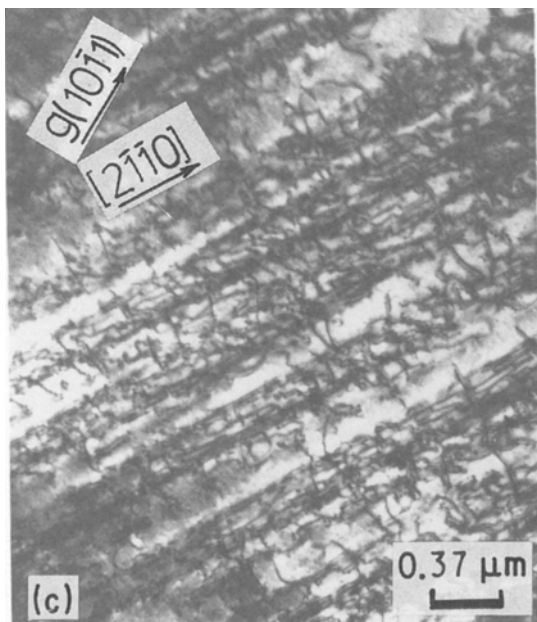
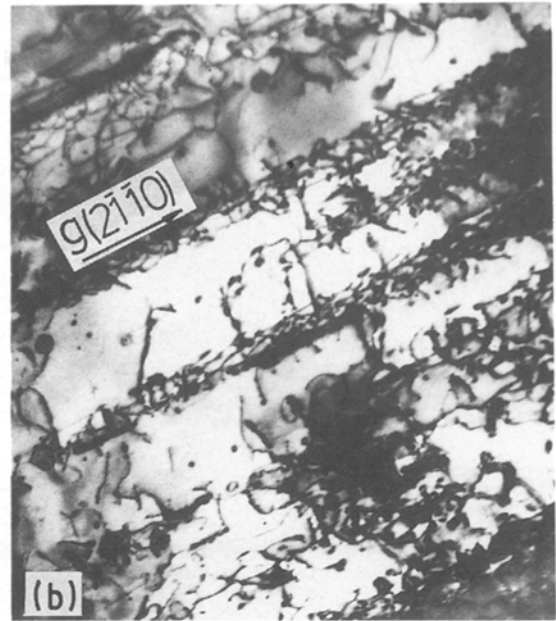
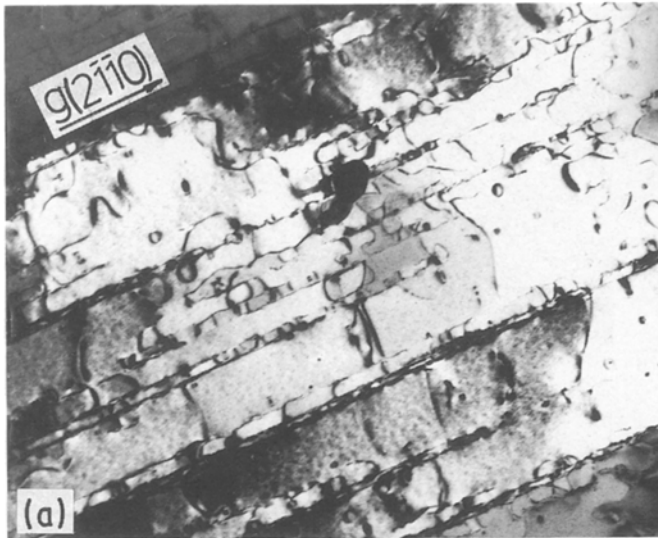


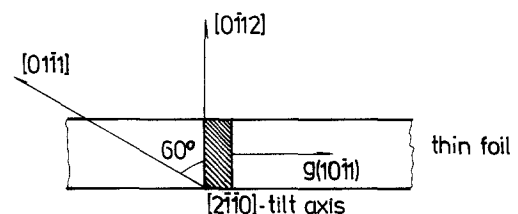
Figure 5 Tilt experiment with $[2\bar{1}\bar{1}0]$ axis: (a) $\bar{B} = [0\bar{1}12] \bar{g}(2\bar{1}\bar{1}0)$, (b) $\bar{B} = [0\bar{1}\bar{1}1] \bar{g}(2\bar{1}\bar{1}0)$, (c) $\bar{B} = [0\bar{1}\bar{1}1] \bar{g}(10\bar{1}1)$.

behaviour show in Fig. 1 suggests that the dislocation structure formed after the first cycle can accommodate the imposed successive plastic strain without significant hardening. As was mentioned above, slip occurs predominately on primary slip system, so that high dislocation density on other planes suggests that at the present condition a process of cross glide may be considered. Moreover, the fact that peak stresses in tension and compression are similar, implies that the dislocation density on slip plane is approximately the same from cycle to cycle. On the other hand, low density of edge components suggests that climb is another important mechanism. In fact,

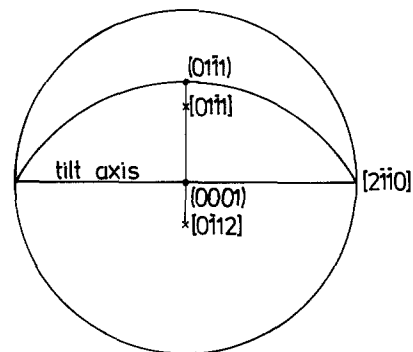
will appear as parallel to the trace of the basal plane, while edge dislocation will appear as normal to the trace of the basal plane. Clearly, the weight which can be placed on such an argument depends upon the extent to which the prism planes may be identified with the operative slip planes. Thus the structure visible on the mentioned directions may be identified as consisting of dense walls of screw dislocations separated by regions of much lower dislocation density containing edge dislocations. Fig. 7 shows a set of micrographs where the beam direction is near to $[0\bar{1}\bar{1}0]$. Here, well straight screw dislocation lies parallel to the trace of the basal plane, so that these defects are entirely confined to their $(0\bar{1}\bar{1}0)$ slip plane. Nevertheless, not all the dislocations conform to this generalization, faint contrast of curved segments lie probably on another plane belonging to the $[2\bar{1}\bar{1}0]$ zone axis.

4. Discussion

From a microstructural point of view, the mechanical



(a)



(b)

Figure 6 Schematic representation from the tilt experiment showed in Fig. 5 (See text).

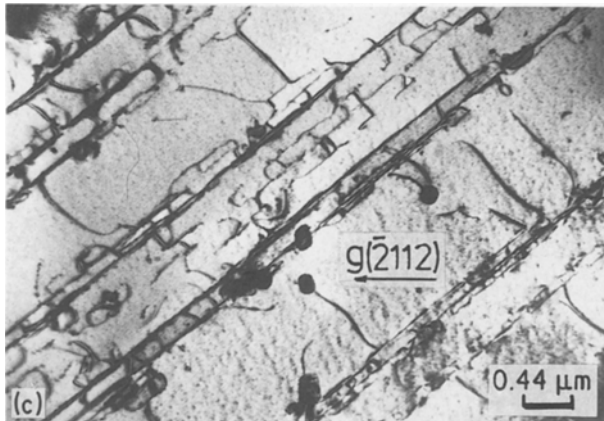
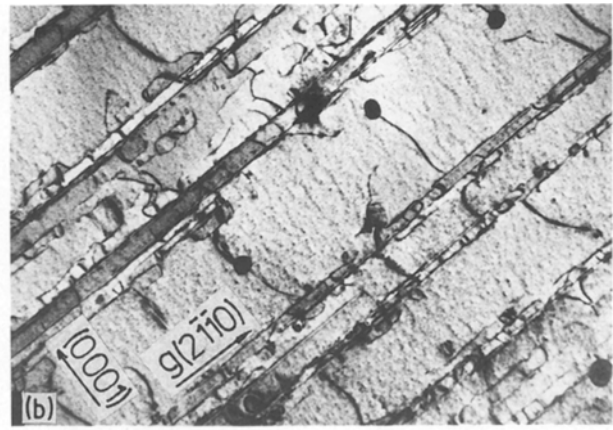
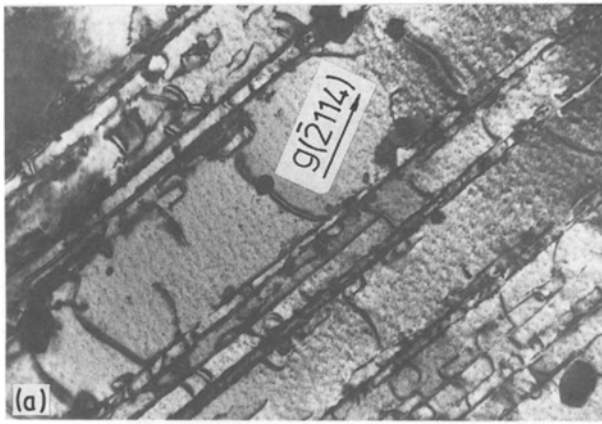


Figure 7 View of the dislocation substructure observed from $\bar{B} = [0\bar{1}10]$.

these two proposed mechanisms are very favourable during high temperature deformation. Bailey [8] has observed by TEM several traces of dislocation movement in Zr at high temperature and has pointed out the climb and dislocation movements to other crystallographic planes are very probable.

Finally, the presence of elongated dislocation loops distributed in some grains at the beginning of cycling and over the band structure is an important feature connected with dislocation processes. The fact that dislocation loops lie along the projection of $\langle 0002 \rangle$ suggests, by geometrical considerations, that they have been formed by intersection of screw dislocations lying on $\langle 10\bar{1}0 \rangle$ planes. In this way, the habit plane of jogs is the prismatic plane. Therefore, they can move conservatively and are able to produce strings or elongated loops of point defects [9].

5. Conclusions

The dislocation substructure induced by strain-controlled LCF tests with $\Delta\epsilon_i = 1\%$ at 873 K in Zircaloy-4 consists of well developed band structure.

The results of trace analysis in concordance with the behaviour of the cyclic stress response led to the conclusion that glide dislocations are able to relieve stress

concentrations by climb and cross slip processes. Therefore, the activation of these two mechanisms, helped by the high mobilities of point defects, compensates the generation of dislocations in each cycle.

Acknowledgements

The authors would like to thank Professor Dr. M. Bocek for his comments and discussions on the present work. This work was done within the Special Intergovernmental Agreement between Argentina and the Federal Republic of Germany and was supported in part by CONICET and the "Proyecto Multinacional de Tecnologia de Materiales", OEA-CNEA.

References

1. J. R. HANCOCK and J. C. GROSSKREUTZ, *Acta Metall.* **17** (1969) 77.
2. C. E. FELTNER and C. LAIRD, *Acta Metall.* **15** (1967) 1621.
3. A. PLUMTREE, Proceedings of the 2nd International Conference on "Low Cycle Fatigue and Elasto plastic Behavior of Materials", Edited by K. T. Rie (Elsevier, Munich, 1987) p. 19.
4. I. ALVAREZ-ARMAS and A. F. ARMAS, "Proceedings of the 2nd International Conference on Low Cycle Fatigue and Elastoplastic Behavior of Materials, Edited by K. T. Rie (Elsevier, Munich, 1987) p. 77.
5. A. F. ARMAS and I. ALVAREZ-ARMAS, "Cyclic Behavior of Zircaloy-4 at Elevated Temperature" (ASTM-STP 1985) p. 617.
6. J. W. EDINGTON, "Practical Electron Microscopy in Materials Science" (The Macmillan Press, London, 1977).
7. R. STEVENSON and J. F. BREEDIS, *Acta Metall.* **23** (1975) 1419.
8. J. E. BAILEY, *J. Nucl. Mater.* **7**, 3 (1962) 300-10.
9. J. WEERTMAN and J. R. WEERTMAN, "Elementary Dislocation Theory" (Macmillan Series in Materials Science, New York, 1967).

Received 20 November 1988
and accepted 31 May 1989